The MMS Fluxgate Magnetometers

Science Data Products Guide

Issue 1.0

Issue Date April 20, 2016

Prepared by: Hannes K. Leinweber, Kenneth R. Bromund, Robert J. Strangeway and Werner Magnes

Approved by: Christopher T. Russell, Robert J. Strangeway, Werner Magnes, Kris Larsen, Mark Chutter, Kenneth R. Bromund and Ferdinand Plaschke

Change Record

Issue	Date	Author	Modifications
Draft 0.7	April 1, 2013	Leinweber	Initial Version
Draft 0.7a	Sept 26, 2013	Bromund	Modifications to file contents, standardized some variable names. Added cal file format.
Draft 0.7b		Bromund	Updates to file contents.
Draft 0.8	March 22, 2014	Leinweber	Changed the description of the guide and calibrations
Draft 0.9	September 6, 2014	Leinweber	Major changes according to SODAWG outline and examples
Draft 0.9a	March 30, 2016	Leinweber, Bromund	Changes according to experience gained from flight data. Update to L2 variable names.
Draft 0.9b	April 01, 2016	Leinweber	Changes made to “Coordinate Systems”
Draft 0.9c	April 05, 2016	Strangeway	Top level changes
Draft 0.9d	April 06, 2016	Leinweber	Some minor changes
Draft 0.9e	April 07, 2016	Leinweber	Changes according to received feedback from team members
Draft 0.9f	April 13, 2016	Bromund	Revised section “Quick-Look Data Products”
Draft 0.9f	April 13, 2016	Leinweber	Rev. section “Instrument Requirements” and minor changes
Draft 0.9f	April 19, 2016	Bromund	Rev. section “Descriptions of L2 Products”
Draft 0.9f	April 20, 2016	Leinweber	Some minor corrections and changes

Table of Contents

1. Introduction

The fluxgate magnetometer (FGM) instrument on board MMS consists of eight individual magnetometers, with two per spacecraft. For each spacecraft one of the magnetometers is known as the Analog Fluxgate (AFG) magnetometer, the other as the Digital Fluxgate (DFG) magnetometer. Flying both the AFG and DFG magnetometers provides redundancy, but, in addition, the overall calibration of the instrument is significantly enhanced by inter-calibrating all eight magnetometers. This is essential for data quantities derived from the level 2 data, such as current densities, that require high precision measurements. In terms of data products, the level 2 products, which use the full inter-magnetometer calibration, have the acronym FGM (fluxgate magnetometer). The lower-level data products are treated separately and use the AFG and DFG acronyms, as these data are not yet combined into the final data product, but are intermediary products.

The AFG and DFG are a part of the FIELDS instrumentation suite (Torbert et. al., 2014) on MMS that provides comprehensive measurements of the full vector magnetic and electric fields in the reconnection regions investigated by MMS, including the dayside magnetopause and the night-side magnetotail acceleration regions out to 25 Re. The FIELDS magnetic sensors consist of redundant flux-gate magnetometers (AFG and DFG) over the frequency range from DC to 64 Hz, a search coil magnetometer (SCM) providing AC measurements over the full whistler mode spectrum expected to be seen on MMS, and an Electron Drift Instrument (EDI) that calibrates offsets for the magnetometers. The FIELDS three-axis electric field measurements are provided by two sets of biased double-probe sensors (SDP and ADP) operating in a highly symmetric spacecraft environment to reduce significantly electrostatic errors. These sensors are complemented with the EDI electric measurements that are free from all local spacecraft perturbations. Cross-calibrated vector electric field measurements are thus produced from DC to 100 kHz, well beyond the upper hybrid resonance whose frequency provides an accurate determination of the local electron density. Due to its very large geometric factor, EDI also provides very high time resolution (~ 1 ms) ambient electron flux measurements at a few selected energies near 1 KeV.

1.1. MMS Science Background

The prime purpose of the MMS mission is to make in-situ measurements of magnetic reconnection. The formation of the four spacecraft is a high quality tetrahedron at the regions where reconnection is expected to occur (dayside and nightside reconnection regions). The

chosen size of the tetrahedron is comparable to the dimensions of the electron diffusion regions (10's of kilometers) so that the motions and sizes of diffusion regions can be determined. Magnetic reconnection is expected to take place inside the diffusion regions. The inter-spacecraft separations of the MMS mission are much smaller compared to the ESA Cluster mission that has separations of ≥ ~100 km.

2. Tri-axial Fluxgate Magnetometers

The magnetic field measurements on each spacecraft are acquired using two tri-axial fluxgate magnetometers (Russell et. al. 2014), one of each mounted on the end of two 5-m booms, each connected to an electronics unit on the main body of the spacecraft, one provided by the Space Research Institute of the Austrian Academy of Sciences, the Digital Fluxgate (DFG), and the other provided by the University of California, Los Angeles, the Analogue Fluxgate (AFG). The instruments form a synchronized, redundant, cross- and inter-spacecraft calibrated pair of magnetometers on each observatory.

2.1. FGM Science Background (from Russell et. al. 2014)

Early measurements of the magnetosphere were principally concentrated in one of three orbits: low-altitude polar, geostationary, and high-altitude elliptical, near the equator. Such missions included the early Interplanetary Monitoring Platforms (IMP) spacecraft, the Advanced Technology Satellites (ATS) series, and the Orbiting Geophysical Observatories (OGO) spacecraft. The odd numbered spacecraft of this latter series were highly elliptical and were launched in 1964, 1966, and 1968. The last highly elliptical mission, OGO-5, worked very well and allowed the detection of the response of the magnetopause to southward fields, which was referred to as erosion, and the reconfiguration of the magnetotail at times of substorms. These observations in turn led to a model of the substorm in which the southward turning of the magnetic field transferred magnetic flux to the geomagnetic tail and then reconnection in the geomagnetic tail led to the return of that flux to the dayside (McPherron et al. 1973; Russell and McPherron 1973). This became known as the near- Earth neutral point model for substorms, but obtaining definitive evidence for reconnection that would convince the skeptics remained elusive, in part because the magnetospheric boundaries were in constant motion and the predicted flows at the magnetopause were orthogonal to the look direction of the detectors that were oriented in the spin plane of the spacecraft. In 1977, a mission to solve these two problems was launched, called the International Sun Earth Explorers 1 and 2. These

two spacecraft co-orbited in a high-altitude elliptical orbit with an adjustable separation. This configuration allowed the motion of the boundary to be measured and the precise distances and thickness of boundaries to be measured. ISEE-1 also had a detector measuring the flow in the north-south direction. Then finally, Paschmann et al. (1979) announced that the flow predicted by reconnection theory was present, and reconnection became accepted by the community as the principal mechanism for energizing the Earth's magnetosphere, albeit with a strident minority opposing this mechanism well into the 21st century. While ISEE 1 and 2 were a breakthrough pair of spacecraft in establishing the existence of reconnection, two spacecraft are not enough to determine the currents flowing in these boundaries. The next major mission, the International Solar Terrestrial Program, was another multi-spacecraft mission, placing three spacecraft in widely separated orbits. This was good for dynamics but not good for microphysics. The Polar spacecraft was a high-altitude elliptical orbiter whose line of apsides precessed around the Earth, with single-spacecraft measurements of reconnection on the tail-lobe magnetopause near the polar cusp and in the near-Earth tail. Also its companions, Geotail and Wind, as well as some other "independent" spacecraft like AMPTE/IRM and Equator-S furthered our understanding of the reconnection process in the magnetotail and at the magnetopause, mainly because of much improved particle instrumentation. But all relied on single spacecraft observations of this highly dynamic and complex process and were thus unable to clearly separate spatial and temporal effects. In 2000, Cluster became the first four-spacecraft mission launched into an orbit similar to that of Polar. It was originally destined to measure the polar cusp which, while largely unexplored, was not expected to support much reconnection. Somewhat unexpectedly, the Cluster mission became a major contributor to the reconnection problem [e.g. Nakamura et al. 2004]. Clearly reconnection was not just the purview of the subsolar magnetopause, but could occur anywhere anti-parallel magnetic fields would appear. However, Cluster had somewhat limited time resolution and usually larger spacecraft separation, providing insight into reconnection on only the ion scale, barely approaching the more important electron scale needed in the electron-diffusion region. Cluster whetted the appetite for a four spacecraft mission to directly address the structure of the reconnection region. Eventually such a mission was approved by NASA, the Magnetospheric Multiscale mission (MMS), ultimately scheduled to be launched in 2015. Further comparisons of the MMS and Cluster missions are given by Torbert et al. (2014). The science of reconnection is now understood qualitatively. Magnetic field lines are defined by electron motion. To have magnetic fields swap partners so that they become connected to different regions requires that the electrons are prevented from following their earlier path. This can only happen on the electron gyroscale. Hence the magnetic field must be measured precisely over a small region which contains the neutral or reconnection point. Not only does the calculation of the magnetic geometry and the currents require a precise magnetic field measurement at four locations, but many of the other instruments require good local magnetic measurements. The mission cannot

achieve its reconnection objectives without excellent magnetic observations on all four spacecraft. The need to understand magnetic reconnection is the principal driver of the measurement objectives of the MMS magnetometers. Since the mission cannot succeed without accurate magnetic measurements on all four spacecraft, magnetometers with maximum redundancy, with different heritage, and provided by different groups, were included. The sensors are similar, while not identical, but the electronic operating principles are quite different. These data are to be completely shared among the team. There is one processing line. The data are continually being inter-compared. There is one magnetometer team who work together with common goals. The magnetometer provided by the Space Research Institute of the Austrian Academy of Science has been called the Digital Fluxgate magnetometer (DFG), and that provided by the University of California, Los Angeles has been called the Analogue Fluxgate magnetometer (AFG).

2.2. MMS Science Objectives

The goal of the MMS mission is to determine why magnetic reconnection occurs, where it occurs, how it varies, how magnetic energy is coupled into heat and particle kinetic energy, and how this energy is coupled into the surrounding plasma. By measuring with unprecedented high time resolution the critical plasma, field, and energetic particle environment from four closely-spaced spacecraft, MMS will quantify the physics of reconnection along boundary regions of the Earth's magnetosphere. The goal will be achieved by measuring electric and magnetic fields and plasmas within the ion and electron diffusion regions that form when magnetic reconnection occurs. Supporting measurements in the regions adjacent to the ion diffusion region will also be important in determining how the energy released in reconnection is coupled to the surrounding plasma. This data will be obtained by a comprehensive complement of instruments on a cluster of four orbiting spacecraft deployed in a tetrahedral configuration along plasma boundary regions such as the magnetopause and magnetotail neutral sheet. The MMS SMART Suite of instruments will take the science measurements required for the MMS mission to achieve its goals. The following are the science objectives for the MMS SMART IS:

- Determine the role played by electron inertial effects and turbulent dissipation in driving reconnection in the electron diffusion region;
- Determine the reconnection rate and what parameters control it;
- Determine the role played by ion inertial effects in the reconnection process.

2.3. Instrument Requirements

The FGM shall measure the 3 axis DC magnetic field vector in low range to an accuracy of better than or equal to 0.5 nT, with an accuracy goal of 0.1 nT in low range.

2.4. Mission Success

Provide answers to the questions formulated in Section 2.2. (Science Objectives) and in terms of data collection: MMS mission success is reached after collecting high-quality data of 16 reconnection events.

2.5. Instrument Description

AFG and DFG represent a redundant system of magnetometers. Each magnetometer is mounted at the end of its own ~5 meter boom. Their electronics boards are different in design and have different heritage (see Section 2.6). The magnetometers use the same sensor design. The only difference is that the DFG sensors have a tuning capacitor directly mounted onto the sensor. Since the sensors do not contain any active parts, using the same set of sensors for AFG and DFG is not considered a violation of redundancy.

The magnetometers have two measurement ranges, a Low-field range and a High-field range. The magnetic field values at which the change from one range to the other occurs are different for AFG and DFG (see Sec. 2.5.2.1. and 2.5.2.2.) which is helpful for instrument calibration.

2.5.1. Tri-axial Fluxgate Sensors

The essential components of each sensor are two magnetic ring cores, possessing wire windings to drive them into saturation, with another set of wire windings for sensing time varying magnetic flux in the cores, and a set of ambient field canceling wire windings, that enable the feedback mode of operation. Ancillary items include two printed circuit boards (PCB's), a 'pig-tail' harness, armatures and a thermistor. When the sensor is operating in feedback mode, the electronics unit cyclically measures the sense winding signal (which scales with the ambient magnetic field permeating the sensor), drives current in the feedback coils

calculated to cancel the measured field, and then rechecks the resulting sense winding signal, searching for a minimum. The field strength reported to the ground is the feedback coil-generated field strength required to cancel the ambient field at the sensor.

2.5.2. Electronics

The electronics units of the AFG and the DFG represent completely different approaches to build feedback magnetometer electronics. Each design has its strengths and weaknesses compared to the other. If magnetometers that are too similar are put onto the same spacecraft, they may experience similar problems and thus redundancy is reduced. Due to their different design approaches, AFG and DFG provide great redundancy for the MMS magnetic field measurements. The two types of magnetometers will be continuously inter-compared (calibrated) during flight and both are expected to provide excellent data. This would not be possible without having the other type of magnetometer for comparison.

2.5.2.1. Digital Fluxgate Magnetometer (DFG)

The DFG is an innovative digital design that uses the sensor pickup coil as well as the feedback coil as part of a sigma-delta control loop (Magnes et. al. 2003 and 2008). This design can be built extremely small and with low power consumption (e.g. with one less DAC per axis compared to other digital designs and without a discrete bandpass filter that traditional analogue fluxgate magnetometers use). The Magnetometer Front-end ASIC (MFA) was developed in a close cooperation between the IWF magnetometer group and the Fraunhofer Institute for Integrated Circuits. The change of ranges for DFG occurs at 550 nT for increasing field and at 500 nT for decreasing field. Four consecutive spins need to meet this criterion. At these field values glitches in the measurements occur. The noise level for high range is ~100 pT/$\sqrt{\text{Hz}}$ at 1 Hz. In low range the DFG magnetometer can operate in two modes: 1) DEC 32 with noise of ~8 pT/$\sqrt{\text{Hz}}$ at 1 Hz and 2) DEC 64 with noise of ~5 pT/$\sqrt{\text{Hz}}$ at 1 Hz). The frequency response is different for the two modes (see Fig. 1 and 2).

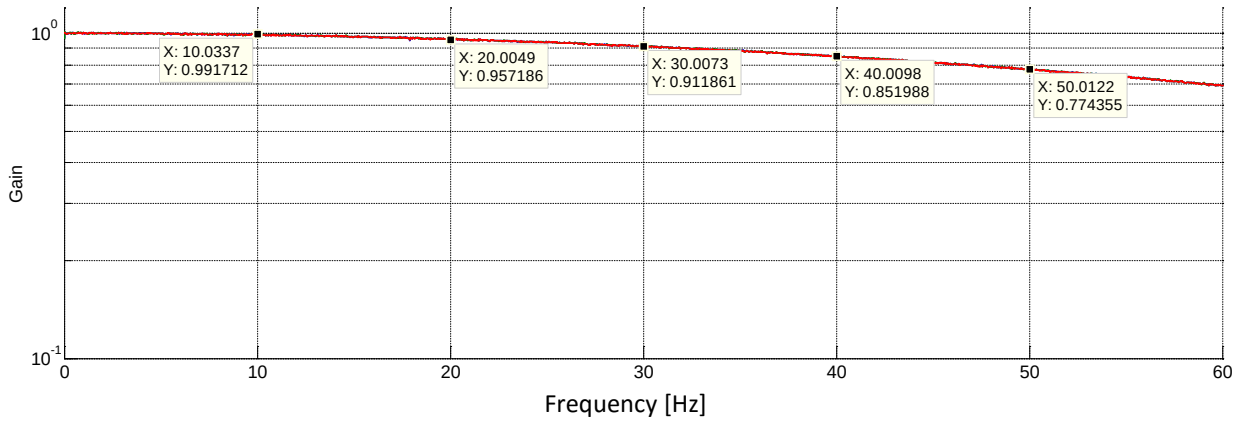

Fig 1. Frequency response for DEC 32 mode of DFG in low range.

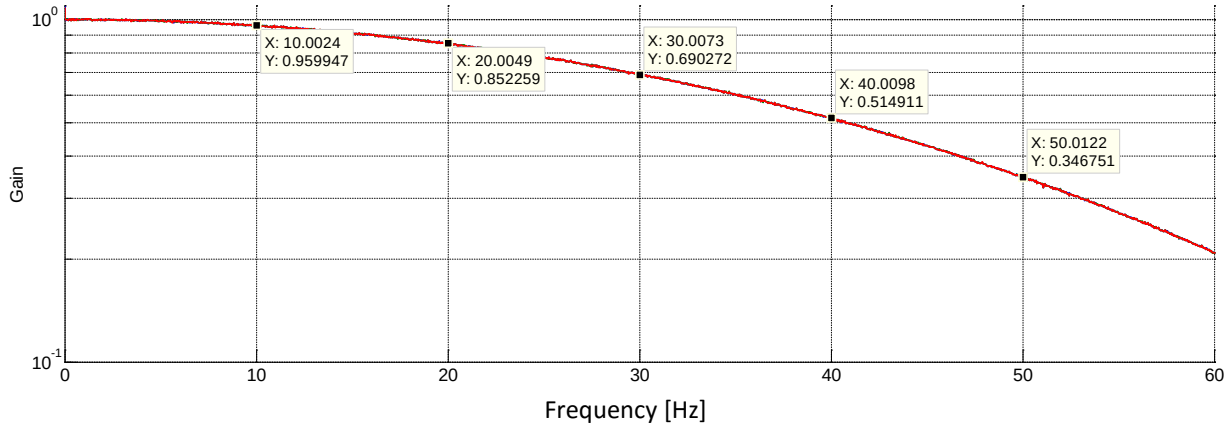

Fig. 2. Frequency response for DEC 64 mode of DFG in low range.

The information whether DFG was in DEC 32 or in DEC 64 mode can be found in the data files (see Sec. 2.9). At the time of writing this feature was not implemented.

2.5.2.2. Analogue Fluxgate Magnetometer (AFG)

The Analogue Fluxgate Magnetometer (AFG) is a traditional design with great heritage that consists of three matched elements, the precision low mass sensor, the interconnecting boom cable, and the electronics board. For optimum operation the electronics and sensor are tuned as a system using an identical interconnecting cable. The change of ranges for AFG occurs at 450 nT for increasing field and at 400 nT for decreasing field. Two consecutive spins need to meet this criterion. At these field values glitches in the measurements occur. The noise level for high range is ~10 pT/$\sqrt{\text{Hz}}$ at 1 Hz and ~5 pT/$\sqrt{\text{Hz}}$ at 1 Hz for low range. The frequency response for low range is given in Fig. 3.

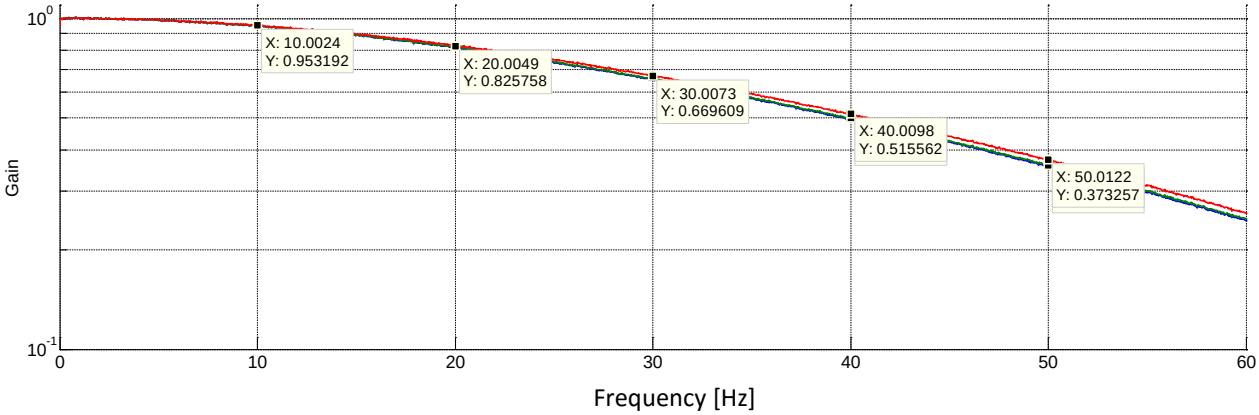

Fig. 3. Frequency response of AFG in low range.

2.6. Heritage

AFG Instrument heritage derives from many previous missions. DFG represents a new development.

2.7. Coordinate Systems

MMS coordinate systems are precisely defined in (461-SYS-SPEC-0115C, or newest version). Below we provide simplified explanations for convenience that should satisfy most users.

2.7.1. Despun Major Principal Axis of inertia (DMPA) coordinates

Data are despun using information about the phase angle so that the Sun lies in the XZ-plane. Z is closely aligned with the spacecraft spin axis. Positive Z is towards north. This coordinate system is mainly used for calibration purpose.

2.7.2. Body Coordinate System (BCS)

This is a coordinate system that spins with the spacecraft and is fixed relative to the spacecraft body. This coordinate system is intended for engineering purposes and is described in 461-SYS-SPEC-0115C, or newest version.

2.7.3. Geocentric Solar Ecliptic (GSE) Coordinates

X lies along the Earth-Sun line. Z is perpendicular to the ecliptic plane towards north. Y is completing the right handed system.

2.7.4. Geocentric Solar Magnetospheric (GSM) Coordinates

X lies along the Earth-Sun line. The dipole axis is within the XZ-plane. Z is directed roughly towards magnetic north. Y is completing the right handed system (and is perpendicular to the dipole axis).

2.7.5. GSM-DMPA Coordinates

This coordinate system is used for Quick-Look data (see Sec. 2.8.).

2.8. Quick-Look Data Products

Quicklook data have the best available calibration at the time of downlink applied and are not intended for scientific analysis.

Quicklook provides time series plots in .png format of FGM data, which is derived from either DFG or AFG.

Magnetic field data is provided in Despun Major Principal Axis of inertia (DMPA) coordinates, which is considered to be a 'near-GSE' coordinate system. That is, no attitude data has been applied, other than to despin using the on-board sun pulse times. The DMPA Z-axis is the aligned with the Major Principal Axis (MPA). In nominal operations, the MPA is maintained to be within 3 degrees of the GSE Z-axis (ecliptic normal). Thus, within the Region of Interest (ROI), DMPA should be within 3 degrees of alignment with true GSE coordinates. The MPA can

be assumed to fixed in inertial space and aligned with the Angular Momentum vector, except in the presence of nutation. For the first year since launch, nutation has been observed to be minimal, and generally damped within hours after spacecraft maneuvers.

In addition, a GSE to GSM transformation is applied to the DMPA data to yield data in what is termed GSM-DMPA coordinates. For a formal discussion of coordinate systems, see the MMS Project Coordinate System and Alignment Document (461-SYS-SPEC-0115C, or most recent version).

2.9. Science Data Products

2.9.1. File Conventions

All science parameters are in CDF files. The CDF files are formatted and named according to the MMS file name conventions (see MMS CDF File Format Guide).

- version will be vX.Y.Z. General MMS guidelines are summarized here, with along with notes of how the FGM specifically interprets these guidelines.
    - X is the interface number. Increments in this number represent a significant change to the format of the file has been made. E.g. new parameters added, or parameters re-named. Also increments upon significant change in the algorithm of the processing software.
    - Y is the quality number. This number represents a change in the quality of the data in the file, which would require re-processing of previously processed data. FGM has a slightly non-standard usage of the Y quality number:
        - Y is the calibration version number.
        - The data file's Y version number corresponds to the Y version number of the calibration file used to generate the data file. The Y version number corresponds to the sequence number of the Magnetometer Conference at which the new calibration file is released.
        - Y does not reset to 0 when X increments.
        - The calibration file Y version number is incremented each time new calibrations are added to the end of the calibration file. Thus, for data files, an increment in Y does not necessarily imply a change in calibration, if earlier data happens to be re-processed after a later calibration is released.
    - Z is the revision number. Z is set to 0 the first time a given file is processed, and is incremented each time the file is re-processed for any reason. Z is reset to 0 after X or Y is incremented.

2.9.1.1. Survey File Conventions

The survey data files combine Slow Survey and Fast Survey data into a single data product. Slow Survey data are measured outside the region of interest (ROI) and are downlinked with eight samples per second. Fast Survey data are measured inside the region of interest and are downlinked with 16 samples per second. Fast Survey data will be available roughly 50 percent of the time per orbit.
Survey files start at with the first complete packet following the even 00:00:00.000 UTC day boundary, so the file names can be uniquely specified by the Year, Month and Day (yyyyMMdd) of the file start time.

2.9.1.2. Burst File Conventions

Burst data are measured inside the region of interest at specific times and are downlinked with 128 samples per second.

There is one burst file for each contiguous burst. There may be more than one burst file per day, so the name of the burst file specifies the start time of the burst, rounded down to the nearest second: yyyyMMddHHmmss.

2.9.2. Descriptions of L2 Products

FGM Level 2 science products use the best available calibration applied that is available 26 days after receipt. However, revised L2 products will be released if significantly better calibrations become available later in the mission. The rather involved calibration procedure is briefly outlined in the Appendix of this document. The Level 2 files to not contain the abbreviations “AFG” or “DFG”, instead “FGM” is being used. The data files are processed with final ephemeris, attitude and spin phase information. L2 data are available from 2015, Sep. 01 onwards.

The FGM data product combines the DFG and AFG data into a single data product, choosing the best data suited for general science. The L2 FGM survey data is taken from the AFG due to consistent low noise (low and high range), but because of the linear phase response (constant group delay) of the DFG, L2 FGM burst data is taken from the DFG.

In addition to the magnetic field measurements, the files contain ephemeris information provided at the intrinsic FDOA product resolution (30 sec). Cubic spline interpolation may be

used to interpolate the ephemeris data to the times of the magnetic field measurements for the purpose of deriving spacecraft separation vectors. Enough ephemeris data will be included to allow for proper interpolation of the ephemeris vectors to each magnetic field vector contained within the file. L2 burst and L2 survey data files will always contain at least two ephemeris data points before the start of the data and two ephemeris data points after the end of the data. For example, even if the duration of a burst is only a few seconds, the data file will contain at least 4 ephemeris data points (2 minutes of ephemeris) to allow for a proper cubic spline fit. This may lead to data overlap when concatenating consecutive bursts, but as each burst is downloaded and processed separately, in order for the ephemeris data to always be useful, each burst file must be treated as if there will be no consecutive bursts. [Note: as of 2015/4/18, only one ephemeris vector is guaranteed before and after the magnetometer data. In the worst case, there may be only 2 or 3 ephemeris data points in a short burst file.]

In the file and parameter names that follow, the first element is always the spacecraft identifier, where mms# stands for mms1, mms2, mms3 or mms4.

2.9.2.1. Survey Data

File names:

mms#_fgm_srvy_l2_yyyyMMdd_vX.Y.Z.cdf

Average data volume per file:

68 MB

2.9.2.2. Burst Data

File Names

mms#_fgm_brst_l2_yyyyMMddHHmmss_vX.Y.Z.cdf

Expected data volume per file:

Largely dependent on SITL decision making. For first 6 months of science phase, Average burst file size was about 1 MB, with an average of 27 burst files per day.

The parameters in each CDF file are summarized in tables 3, 4 and 5. Table 3 lists the names of the magnetic field data parameters. Table 4 lists the magnetic field housekeeping parameters that are designated as VAR_TYPE = ‘support_data’.

The content of Burst and Survey files are the same. For the Burst parameter names and labels, replace '_srvy' with '_brst' in Tables 3-5.

Table 3. L2 Magnetic Field Time Series data parameters. All parameters have VAR_TYPE = 'data'. For burst files, replace '_srvy' with '_brst' in the parameter names and labels.

Name	Type	Dimension	Labels [description]	Unit
Epoch	CDF_TIME_TT2000	0:[]	TT2000	Nanoseconds, epoch terrestrial time J2000
mms#_fgm_b_gse_srvy_l2	CDF_REAL4	1:[4]	Bx GSE, By GSE, Bz GSE, Bt	nT
mms#_fgm_b_gsm_srvy_l2	CDF_REAL4	1:[4]	Bx GSM, By GSM, Bz GSM, Bt	nT
mms#_fgm_b_dmpa_srvy_l2	CDF_REAL4	1:[4]	Bx BCS, By BCS, Bz BCS, Bt	nT
mms#_fgm_b_bcs_srvy_l2	CDF_REAL4	1:[4]	Bx DMPA, By DMPA, Bz DMPA, Bt	nT

Table 4. L2 Housekeeping data parameters associated record-for-record with the magnetic field data. (* indicates parameters with VAR_TYPE = 'support_data'). For burst files, replace '_srvy' with '_brst' in the parameter names and labels.

Name	Type	Dimension	Labels [description]	Unit
mms#_fgm_flag_srvy_l2 *	CDF_UINT4	0:[]	mms#_fgm_flag_srvy_l2 *	0=good. See Table 6 for bit definitions
mms#_fgm_hirange_srvy_l2 *	CDF_UINT1	0:[]	mms#_fgm_hirange_srvy_l2 [high/low magnetic field range]	1=high range, 0=low range
mms#_fgm_stemp_srvy_l2 *	CDF_FLOAT	0:[]	mms#_fgm_stemp_srvy_l2 [sensor temperature]	C
mms#_fgm_etemp_srvy_l2 *	CDF_FLOAT	0:[]	mms#_fgm_etemp_srvy_l2 [electronics temperature]	C
mms#_fgm_mode_srvy_l2 *	CDF_FLOAT	0:[]	mms#_fgm_mode_srvy_l2 [Unambiguously identifies fast, slow or f128 as the source data mode of a given record. NOTE: for srvy data, instrument modes with more than 16 S/s are decimated to 16 S/s]	Samples/s
mms#_fgm_bdeltahalf_srvy_l2 *	CDF_FLOAT	0:[]	mms#_fgm_bdeltahalf_srvy_l2 [1/2 delta-t for B-field data]	s

Table 5. L2 CDF File ancillary parameters: (* Indicates parameter VAR_TYPE is 'support_data') For burst files, replace '_srvy' with '_brst' in the parameter names and labels.

Name	Type	Dimension	Labels	Unit
Epoch_state	CDF_TIME_TT2000	0:[]	TT2000 [time tags for ephemeris data]	Nanoseconds, epoch terrestrial time J2000
mms#_fgm_r_gse_srvy_l2	CDF_REAL4	1:[4]	X GSE, Y GSE, Z GSE, R	Km
mms#_fgm_r_gsm_srvy_l2	CDF_REAL4	1:[4]	X GSM, Y GSM, Z GSM, R	Km
mms#_fgm_rdeltahalf_srvy_l2 *	CDF_FLOAT	0:[]	mms#_fgm_rdeltahalf_srvy_l2 [1/2 delta-t for ephemeris data]	s

2.9.3. Quality Control and Diagnostics

Data are flagged by automated algorithms that detect glitches due to change in gain at range change boundaries, instrument saturation, and other known and defects. In addition, there is a facility to manually flag data which has been determined to be bad. Table 6 summarizes the flags that are applied to the data.

Table 6. Data flags in mms#_fgm_flag_srvy_l2 and mms#_fgm_brst_l2. Bits marked TBD are reserved to identify future potential problems. The default action of all software should be to blank all data where any of the flag bits are set.

Bit	Flag Definition
0	TBD
1	TBD
2	User Flagged
3	TBD
4	B1 saturated
5	B2 saturated
6	B3 saturated
7	Range-change glitch
8-31	TBD

2.9.3.1. Error Analysis

The global TEXT attribute of each CDF includes a description of the estimated error in nT.

References

Khurana, K. K., E. L. Kepko, M. G. Kivelson, and R. C. Elphic, Accurate determination of magnetic field gradients from four point vector measurements: 2. Use of natural constraints on vector data obtained from four spinning spacecraft, IEEE T. Magn. 32, 5193, 1996.

Leinweber, H. K., C. T. Russell, K. Torkar, T. L. Zhang, and V. Angelopoulos, An advanced approach to finding magnetometer zero levels in the interplanetary magnetic field, Meas. Sci. Technol. 19(5), 2008.

Leinweber, H. K., In-flight Calibration of Space-borne magnetometers, PhD Thesis, Graz University of Technology, 2012.

Leinweber, H. K., C. T. Russell, and K. Torkar, Precise Calculation of Current Densities via Four Spinning Spacecraft in a Tetrahedron Configuration, IEEE Trans. Magn., 49, 5264, 2013

Magnes W., Pierce D., Valavanoglou A., Means J., Baumjohann W., Russell C. T., Schwingenschuh K. and Graber G., A sigma-delta fluxgate magnetometer for space applications, Meas. Sci. Technol. 14 1003–12, 2003.

Magnes W., M. Oberst, A. Valavanoglou, H. Hauer, C. Hagen, I. Jernej, H. Neubauer, W. Baumjohann, D. Pierce, J. Means and P. Falkner, Highly integrated front-end electronics for spaceborne fluxgate sensors, Meas. Sci. Technol. 19 115801 doi:10.1088/0957-0233/19/11/115801, 2008.

McPherron, R. L., Russell, C. T., and Aubry, M. P., Satellite studies of magnetospheric substorms on August 15, 1968. IX. Phenomenological model for substorms: J. Geophys. Res., v. 78, p. 3131-3149, 1973.

Nakamura R. F., W. Baumjohann, C. Moulkis, L. M. Kistler, A. Runov, M. Volwerk, Y. Asano, Z. Voros, T. L. Zhang, B. Klecker, H. Reme, A. Balogh, Spatial scale of high-speed flows in the plasma sheet observed by Cluster, Geophys. Res. Lett. (2004). doi:10.1029/2004GL019558

Paschmann, G., Sonnerup, B. U. Ö., Papamastorakis, I., Sckopke, N., Haerendel, G., Bame, S. J., Asbridge, J. R., Gosling, J. T., Russell, C. T., and Elphic, R. C., Plasma acceleration at the Earth's magnetopause: Evidence for reconnection: Nature, v. 282, p. 243-246, 1979.

Plaschke F., R. Nakamura, H. K. Leinweber, M. Chutter, H. Vaith, W. Baumjohann, M. Steller and W. Magnes, Flux-gate magnetometer spin axis offset calibration using the electron drift instrument. Meas. Sci. Technol., 25, 105008, doi:10.1088/0957-0233/25/10/105008, 2014.

Russell, C. T., McPherron, R.L., The magnetotail and substorms: Space Sci. Rev., v. 15, p. 205-266, 1973.

Russell C. T., B. J. Anderson, W. Baumjohann, K. R. Bromund, D. Dearborn, D. Fischer, G. Le, H. K. Leinweber, D. Leneman, W. Magnes, J. D. Means, M. B. Moldwin, R. Nakamura, D. Pierce, F. Plaschke, K. M. Rowe, J. A. Slavin, R. J. Strangeway, R. Torbert, C. Hagen, I. Jernej, A. Valavanoglou, I. Richter, The Magnetospheric Multiscale Magnetometers, Space Sci. Rev., DOI 10.1007/s11214-014-0057-3, 2014.

Torbert R. B., C.T. Russell, W. Magnes, R.E. Ergun, P.A. Lindquist, O. LeContel, H. Vaith, J. Macri, S. Myers, D. Rau, J. Needell, B. King, M. Granoff, M. Chutter, I. Dors, G. Olsson, Y. Khotyaintser, A. Erikson, G.A. Kletzing, S. Bounds, B.J. Anderson, W. Baumjohann, M. Stellar, K. Bromund, G. Le, R. Nakamura, R.J. Strangeway, S. Tucker, J. Westfall, D. Fisher, F. Plaschke, The FIELDS Instrument Suite on MMS: Scientific Objectives, Measurements, and Data Products., Space Sci. Rev., DOI 0.1007/s11214-014-0109-8, 2014.

Appendix

A.1. Instrument Calibration

There are two main types of calibrations for space-borne magnetometers, namely ground calibrations and in-flight calibrations. Ground calibrations have a dual purpose. They provide a valuable functional test, and determine all twelve calibration parameters. Furthermore, the ground tests provide insights on temperature dependence, linearity and timing. Most importantly, these tests occur in a controlled environment and cover the full range of expected conditions of temperature and field strength. In-flight calibrations are needed to precisely adjust calibration parameters for the encountered conditions on orbit as well as capturing changes of calibration parameters that are less stable. These calibrations are valuable as they occur close in time to the acquisition of the science data, but they are not obtained in a controlled environment. For example, the field magnitude, the field direction, and the temperature may be changing simultaneously. A linear magnetometer can be calibrated with the twelve calibration parameters defined below. The parameters consist of three gains, three offsets and six angles (see Fig. A1).

$$\begin{pmatrix} B_{S_1} \\ B_{S_2} \\ B_{S_3} \end{pmatrix} = \begin{pmatrix} G_1 \sin\theta_1 \cos\varphi_1 & G_1 \sin\theta_1 \sin\varphi_1 & G_1 \cos\theta_1 \\ G_2 \sin\theta_2 \cos\varphi_2 & G_2 \sin\theta_2 \sin\varphi_2 & G_2 \cos\theta_2 \\ G_3 \sin\theta_3 \cos\varphi_3 & G_3 \sin\theta_3 \sin\varphi_3 & G_3 \cos\theta_3 \end{pmatrix} \cdot \begin{pmatrix} B_x \\ B_y \\ B_z \end{pmatrix} + \begin{pmatrix} O_1 \\ O_2 \\ O_3 \end{pmatrix}$$

B_{S_1}, B_{S_2}, B_{S_3}	non-orthogonal field components as measured by the magnetometer sensors
B_x, B_y, B_z	orthogonalized field components
G_1, G_2, G_3	gain corrections of each of the sensors
θ_1, θ_2, θ_3	elevation angles of each of the sensors
φ_1, φ_2, φ_3	azimuthal angles of each of the sensors
O_1, O_2, O_3	offsets of each of the sensors

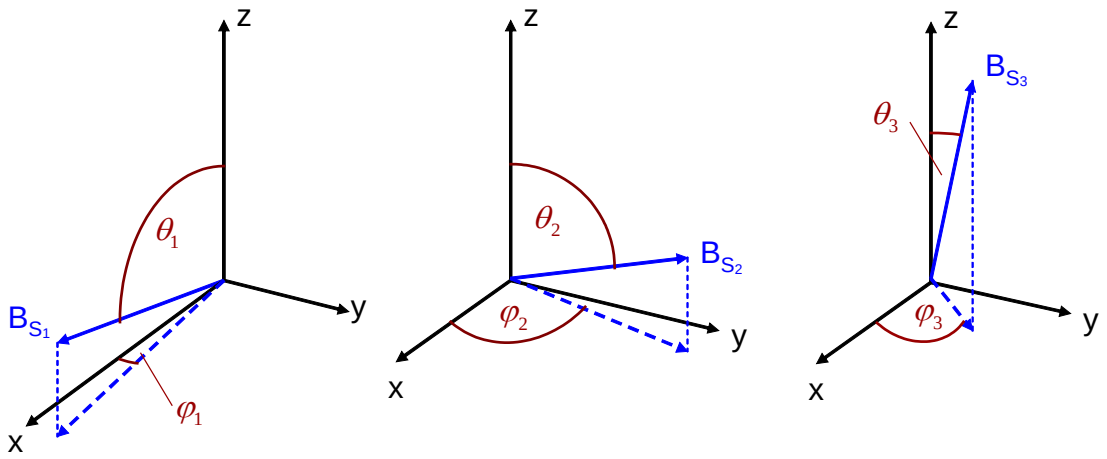

Fig. A1. Definition of six angles for magnetometer calibration. The z-axis is defined as spin axis.

The above matrix is the inverse of a calibration matrix. The six angles describe the orientation of the sensor axes with respect to the sensor mechanical axes. The angles provide information on orthogonality as well as absolute orientation with respect to the mechanical axes.

A1.1. Ground Calibration

All magnetometers went through a variety of ground tests at different magnetic testing facilities of TU-Braunschweig, UCLA, IWF-Graz and UNH (timing tests). The most important parameters that were derived from the ground tests are sensor alignment angles (magnetic) with their mechanical axes (alignment tests also provide orthogonality), gain drifts vs. sensor temperature, gain drifts vs. electronics temperature, linearity, linearity vs. temperature, and synchronization of instrument timing (group delays).

A.1.1.1. Temperature Corrections

Corrections for gains vs. temperature and linearity vs. temperature (DFG) are part of the data processing stream. For each magnetometer, the sensor temperature and the electronics temperature is available from the housekeeping data stream. For spinning spacecraft, orthogonality can be well established in-flight also for varying temperatures (Leinweber, 2012). Sensor offsets are determined by in-flight techniques. Special smoothing algorithms are applied to the sensor temperatures to avoid contaminating the magnetic field data with noise from the temperature sensors.

A.1.1.2. Timing Corrections

Timing corrections (group delays) have been determined on ground and are implemented into the data processing stream.

A1.2. In-Flight Calibration

There are a number of different techniques that can be used to cross check or adjust magnetometer calibration parameters on orbit. Eight out of twelve calibration parameters can be found (with high accuracy) via removal of spin tone in a de-spun coordinate system. The remaining four calibration parameters are calculated using a set of techniques. The set consists of removal of jumps that occur during range changes (Leinweber et. al., 2013), Earth field comparison (Leinweber, 2012), cross calibration with EDI (Plaschke et. al., 2014), cross checks in the solar wind (Leinweber et. al., 2008). MMS will rarely encounter the solar wind. Additionally, inter-spacecraft calibration (Khurana et. al., 1996; Leinweber et. al., 2013) is necessary to further refine the calibration parameters. The overall in-flight calibration plan for producing Level 2 data is outlined in Fig. A2.

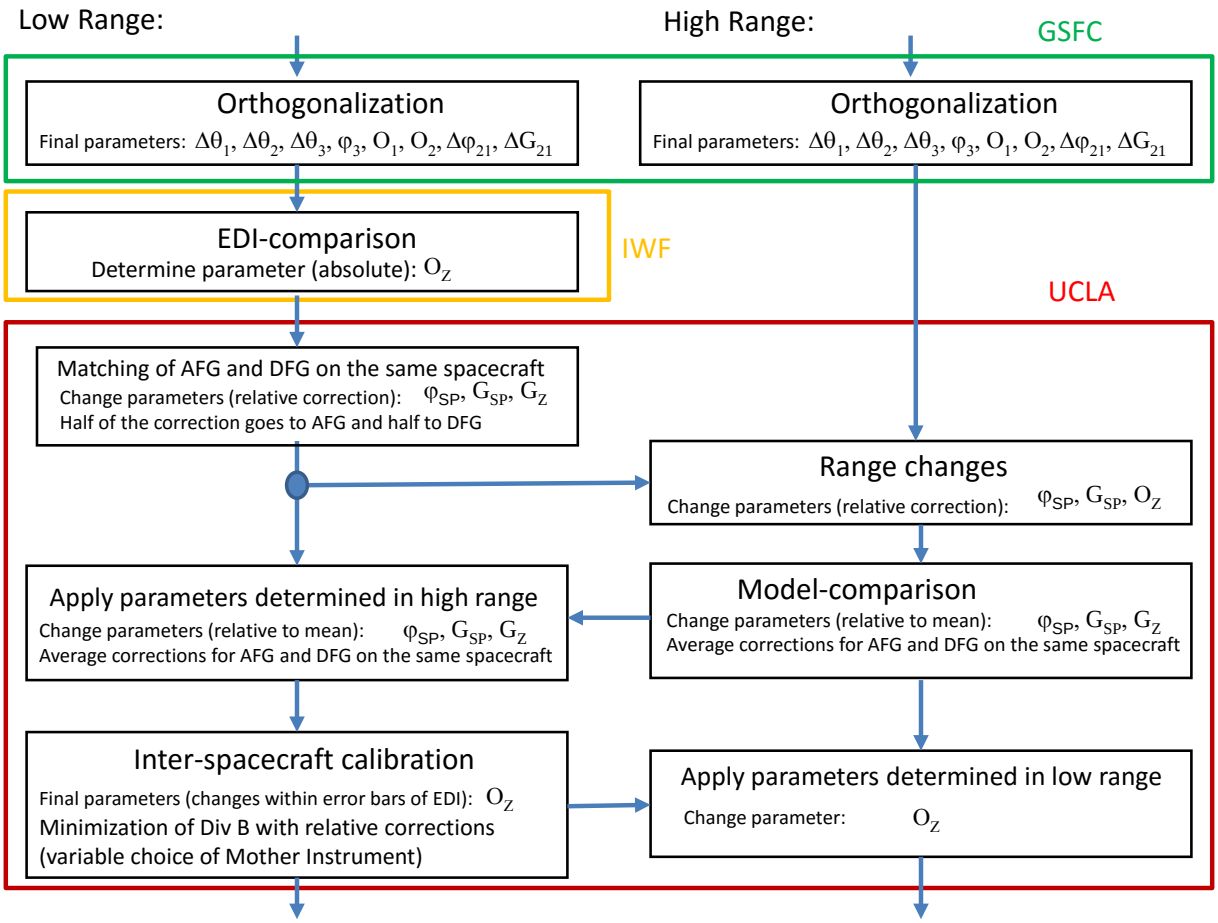

Fig. A2. Outline of the overall AFG/DFG in-flight calibration plan for Level 2 data. For a spinning spacecraft, calibration parameters that are applied to both spin plane sensors are ΔG_{SP}, the spin plane gain correction and $\Delta\varphi_{SP}$ the azimuthal angular correction of both spin plane sensors. G_Z and O_Z are the spin axis gain and spin axis offset.

The MMS in-flight magnetometer calibration is a shared task between UCLA, GSFC and IWF-Graz. All three institutions have clearly defined calibration tasks and work together to provide calibration parameters on a tight schedule. The calibration efforts and results are discussed at a weekly mag-conference between UNH, UCLA, GSFC and IWF-Graz. The calibration flow as outlined in Fig. A2 is a continuous iterative approach to find time varying calibration parameters. The three institutions iterate through the whole process on a tight schedule.